

Results are shown of an experimental and analytical study concerning the heat transfer from an anisothermal jet to a fluidization bed, and a model is proposed to describe this heat transfer.

It is well recognized that, although many studies have been made concerning the heat transfer from the gas to the solid particles in a fluidization bed, no reliable basis for generalizing the heat-transfer coefficients can be counted on. An entirely plausible reason for this is, according to [1], that the mechanism of heat transfer in a fixed bed has been assumed adequate as also mechanism of heat transfer in a fluidized bed, although the modes of gas flow are different in both.

It had been hypothesized earlier [2] that the active zone of heat transfer in a fluidization bed is as high as the jets discharging from the gas distributor grid. This hypothesis was based on the jet model of a fluidization bed, according to which the fluidizing agent flows in two modes: through the interstices between solid particles and as a jet [2, 3, 4]. The appearance of bubbles in a bed and, consequently, the formation of microgaps [5] is related to the peculiarities of jet development in a fluidization bed with a density much higher than that of the gas. The attenuation of turbulent fluctuations during momentum exchange between phases of different densities results in a compression of the jet and its subsequent separation, together with the gas-solid particles zone. The generated bubbles transfer part of the heat beyond the active zone. In order to develop a better model of the heat transfer in a fluidized bed, therefore, it is necessary to learn more about the heat transfer to the bed from both the jets discharging into it and from the ascending bubbles. For this, one must first establish how a single anisothermal jet builds up and how the heat is transferred from it to the bed, and only then one can consider the heat transfer from an array of jets.

The discharge of an anisothermal jet and the heat transfer from it to a bed was studied experimentally in a cylindrical laboratory reactor 125 mm in diameter, made of acrylic glass and containing a bed of granular material fluidized with air. At the center of the gas distributor grid was placed a nozzle, 8 mm in diameter, discharging a jet of air preheated in an electric furnace. The fluidizing air was supplied from a blower without preheating. All tests were performed at a constant bed temperature and, for this purpose, all excess heat was removed through a heat exchanger coil around the bed periphery.

Temperatures and velocities were measured with a special probe which could be moved around through a coordinate-drive mechanism [6] and which included a Pitot-Prandtl pneumometer tube as well as a thermometer tube with a copper-constantan thermocouple inside, the wires of the latter 0.1 mm in diameter butt-welded into a junction. Such a thermocouple layout ensured a steady value of the recovery coefficient up to Mach number $M = 1$. As secondary instrument served a model KP-59 dc potentiometer of accuracy class 0.05, which measured the temperature within 0.5°C . The pneumometric tube was connected to a model MMN cup-type alcohol manometer, for measuring pressure drops to 0.1 mm H_2O - equivalent to an air velocity of 1.2 m/sec.

The jet was discharging into a monodisperse bed of particles with characteristics as listed in Table 1. The jet superheat above the temperature of the fluidizing agent θ was varied from 1.5 to 4.0, while the jet velocity was varied from 20 to 90 m/sec. The tests were performed at a close to minimum operating velocity of the fluidizing agent ($W \approx 2$). The bed height in the apparatus was 100-180 mm.

Institute of Chemical Apparatus Design, Moscow. Translated from *Inzhenerno-Fizicheski Zhurnal*, Vol. 25, No. 4, pp. 581-588, October, 1973. Original article submitted April 19, 1973.

© 1975 Plenum Publishing Corporation, 227 West 17th Street, New York, N.Y. 10011. No part of this publication may be reproduced, stored in a retrieval system, or transmitted, in any form or by any means, electronic, mechanical, photocopying, microfilming, recording or otherwise, without written permission of the publisher. A copy of this article is available from the publisher for \$15.00.

TABLE 1. Characteristic of the Materials Used for the Experiment

Material	Particle size	Minimum fluidization rate	Free lift velocity
Aluminosilicate catalyst	2-2,5	0,85	5,85
The same	2,5-3	0,99	6,41
" "	3-4	1,13	7,26
" "	4-5	1,36	8,2
Glass balls	1-1,6	0,85	5,65
Polystyrene	1,5-2	0,45	4,68
Nitro-ammonium phosphate	1,6-2	0,66	5,88

The hydrodynamic and the thermal boundaries of anisothermal turbulent jets were traced by velocity and temperature measurements along the jet axis and across jet sections.

An analysis of axial temperature and velocity profiles (Fig. 1) indicates that these quantities are continuously decreasing, as a result of momentum and heat transfer from the jet to the surrounding bed. Beginning at a distance approximately equal to one nozzle diameter, the temperature and the velocity both drop sharply; the trend of the curves then changes, they become flatter. At the tip of the air jet, where the air velocity becomes equal to the lift velocity of solid bed particles [2], the temperature at the jet axis remains 2-10°C above the bed temperature. Most typical data on the temperature relaxation at various values of the jet parameters are given in Table 2.

For particles described in Table 1, the temperature relaxation along the jet axis $[(T_0 - T_j)/(T_0 - T_b)]$ is determined not only by the jet discharge velocity corresponding to particles of a given size but also by the ratio of jet length to bed height x_j/l_b (Fig. 2). According to the graph, the temperature relaxation increases with an increasing ratio x_j/l_b and reaches 90-98% when $x_j/l_b \approx 0.7$. It has been suggested earlier [6] that two modes of jet discharge be considered here: local spouting and bubble flow, characterized by different sizes of breakaway bubble and different breakaway frequencies. Local spouting of vertical jets occurs when $x_j/l_b \approx 0.6$ and is characterized by a high rate of regular circulation of solid particles from the jet orifice along the jet boundary into the bed and back, but during transition to the bubble mode this pattern is disturbed. Data on temperature relaxation have confirmed the results of our analysis.

No sharp transition from bubble flow to local spouting was noted, on the other hand, but only a smooth change in the relaxation rate. If 90% or more relaxation is considered sufficient, then the ratio $x_j/l_b = 0.7$ may be regarded as critical; at ratios larger than that the flow changes to local spouting. Beyond the jet boundary the temperature decreases much slower along the jet axis (Fig. 1).

Thus, the rate of interphase heat transfer is highest within the dynamic jet boundaries. Consequently, the active zone referred to by several authors in connection with fluidization apparatus is the

TABLE 2. Results of Temperature Relaxation Measurements at the Tip of a Jet

Material	Initial discharge velocity U_0 , m/sec	Bed height l_b , mm	Initial jet temperature T_0 , °C	Bed temperature T_b , °C	Superheat θ	x_j/l_b	Temperature relaxation, %
Aluminosilicate catalyst	31,3	100	42,6	21,7	1,92	0,5	73,6
2-2.5	42	160	62	21,2	2,9	0,48	85,2
The same	58,1	140	87,2	27,5	3,2	0,95	91,6
Aluminosilicate catalyst							
2,5-3	34,9	100	43,9	16,9	2,6	0,63	89
The same	49,4	180	51,6	16,8	3	0,6	97
	62,3	140	75,5	26,1	2,9	0,83	95,1
Aluminosilicate catalyst							
3-4	32,5	140	55,4	19	2,9	0,31	74
The same	61,9	160	85,6	30,6	2,8	0,6	86,3
Aluminosilicate catalyst							
4-5	39,5	160	30,1	20,2	2,5	0,2	58
The same	41	120	59,3	24,6	2,4	0,43	73
Nitro-ammonium phosphate							
1,6-2	33	180	56,6	18	3,15	0,23	75
The same	38	140	56,6	21,2	2,7	0,6	90,1

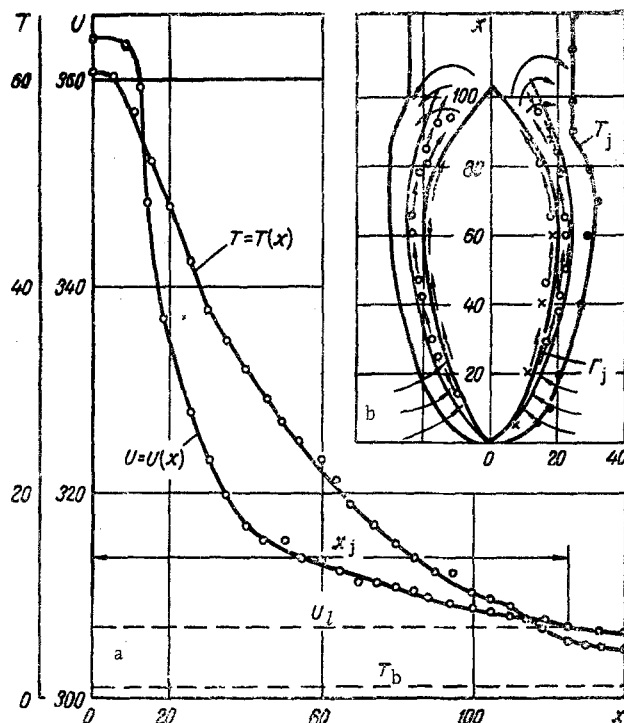


Fig. 1. a) Axial velocity profile (U , m/sec) and temperature profile (T , °K) of a jet (x , mm); b) boundaries of the air jet (Γ_j , mm) and thermal boundaries of the jet (T_j , mm).

zone where jets discharging from the distributor grid spread. The heat-transfer rate within this zone depends not only on the velocity of the fluidizing agent but also on the discharge mode, however, and this mode can be determined from the x_j/l_b ratio. When that ratio is small (e.g., $x_j/l_b = 0.2$), as is often the case in practice, then only approximately half the heat is dissipated within the layer adjacent to the distributor grid and the rest of the heat is carried by the bubbles into the bed core. Of course, some of the heat is undoubtedly transmitted to the bed by the air filtrating from the jet through the interstices between grains.

For this reason, defining the heat-transfer coefficient in terms of the surface of all particles in a bed is just as incorrect as defining it in terms of the surface of all particles in the active zone only. Indeed, an error is introduced in the definition of the heat-transfer coefficient when the heat-transfer surface is calculated as the total surface of particles in the active zone, because not all particles participate equally in the heat transfer: some are engaged in the process after having penetrated into the jet zone, while others are in contact with the filtrating air. On the other hand, calculating the heat-transfer coefficient on the basis of the surface of all particles in a bed seems even less legitimate, inasmuch as the actual heat-transfer surface consists only of the surface of particles within the jet zone and the surface of particles in contact with air bubbles [7, 8].

Temperature and velocity measurements across jet sections have shown that the dynamic and the thermal boundaries first widen with increasing distance from the nozzle, and then narrow down while the velocity and the temperature along the jet axis continuously decrease. It has been established in an analysis of dynamic and thermal boundaries that these boundaries do not coincide dimensionally, the thermal boundaries remaining on the average 1.5 times wider than the dynamic boundaries. Within the dynamic boundaries the heat-transfer proceeds to about 90% completion. This is clearly evident in Fig. 3. The temperature gradient outside the dynamic profile is small. A similar trend is noted during the discharge of free anisothermal jets [9]. The temperature drop outside the dynamic profile is explained by heat conduction and also by air filtration from the jet to the bed core.

Measurements made across the thickness of the dynamic boundary layer were compared with the formula for an isothermal jet according to [2]:

$$b = C_1 \left(\frac{U_m - U_A}{U_m + U_A} + \sqrt{\frac{\rho_l}{\rho_l'}} \right) x. \quad (1)$$

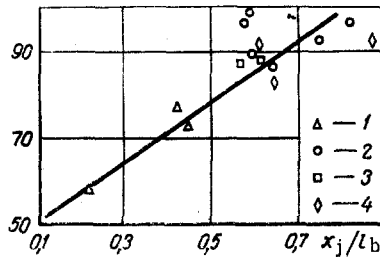


Fig. 2

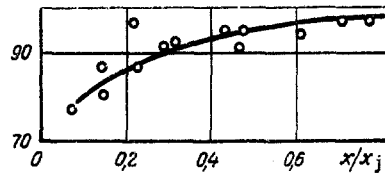


Fig. 3

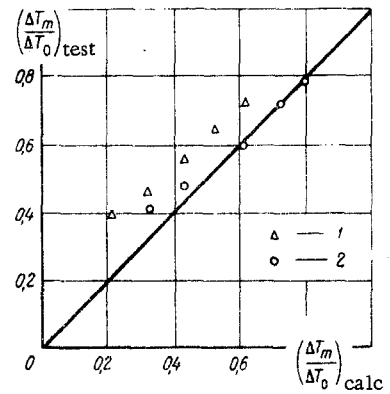


Fig. 4

Fig. 2. Temperature relaxation (%) within the gas jet boundaries, as a function of the ratio x_j/l_b : 1) for aluminosilicate catalyst, $d = 4-5$; 2) $d = 3-4$; 3) $d = 2.0-2.5$; 4) for nitro-ammonium phosphate, $d = 1.6-2.0$.

Fig. 3. Temperature relaxation (%) within the dynamic jet boundaries, across a jet section, as a function of the distance from the discharge orifice.

Fig. 4. Correlation curve: 1) bubble mode; 2) local spouting mode.

Such a comparison has revealed that this formula is also suitable for an anisothermal jet. However, the value of coefficient c_{1n} is higher here than in the case of an isothermal jet. An evaluation of test data has yielded the following empirical relation for this coefficient:

$$C_{1n} = 0.46Ga^{0.10}\theta^{0.20} \quad (2)$$

The profiles of velocity and temperature were evaluated in dimensionless coordinates, with the abscissas referred to the thickness of the dynamic boundary layer. The dimensionless velocities and temperatures were found to be affined, the former clustering closely about a curve described by the G. Schlichting equation [10]:

$$\frac{U}{U_m} = \left[1 - \left(\frac{r}{b} \right)^{1.5} \right]^2 \quad (3)$$

and the latter clustering about a curve described by the Taylor equation:

$$\frac{\Delta T}{\Delta T_m} = 1 - \left(\frac{r}{b} \right)^{1.5} \quad (4)$$

The resulting data on the affinity between velocities and temperatures have yielded an analytical solution to the problem of heat transfer from a jet to a bed. This analysis was based on Prandtl's theory of turbulence and the earlier stated hypothesis concerning the existence of two zones in the boundary layer [2]. We started out with the integral equation of constant excess heat content at any jet section

$$\rho_A c_A r_0^2 U_0 \Delta T_0 = \int_0^b \rho_{ms} c_{ms} U \Delta T 2\pi r dr \quad (5)$$

We divided both sides of this equation by $U_m \Delta T_m b^2$ to obtain

$$\rho_A c_A \frac{r_0^2}{b^2} \cdot \frac{U_0}{U_m} \cdot \frac{\Delta T_0}{\Delta T_m} = 2\rho_{ms} c_{ms} \int_0^1 \frac{U}{U_m} \cdot \frac{\Delta T}{\Delta T_m} \cdot \frac{r}{b} d\left(\frac{r}{b}\right) \quad (6)$$

and then integrated, taking into account expressions (3) and (4) as well as remembering that an average 90% temperature relaxation occurs within the dynamic boundaries of a jet section (Fig. 3). As a result, we obtained the following formula for calculating the temperature drop along a jet axis:

$$\frac{\Delta T_m}{\Delta T_0} = 6.2 \frac{\rho_A}{\rho_{ms}} \cdot \frac{c_A}{c_{ms}} \cdot \frac{U_0}{U_m} \cdot \frac{r_0^2}{b^2} \quad (7)$$

The temperature relaxation within the air jet region can be determined from formula (7), if the boundary conditions at the jet tip are inserted into it: $U_m = U_l$, $c_{ms} = c_{A'}$, $\rho_{ms} = \rho_{A'}$, and $b = C_{in} \sqrt{(\rho_A / \rho_{A'}) x_j}$. The expression then changes to

$$\frac{\Delta T_m}{\Delta T_0} = 6.2 \frac{c_A}{c_{A'}} \cdot \frac{U_0}{U_l} \cdot \frac{r_0^2}{C_{in}^2 x_j^2} \quad (8)$$

However, Eqs. (7) and (8) have been obtained here on the assumption of an almost complete temperature relaxation along the jet. In reality, on the other hand, we have shown here that the relaxation depends on the ratio x_j/l_b . This formula yields a satisfactory agreement with test data when $x_j/l_b \geq 0.8$, therefore, while differences are noted when the value of this ratio is smaller (Fig. 4). In order to utilize the analytical solution for all discharge modes, we have introduced a relaxation coefficient p which, according to our data, depends on the ratio x_j/l_b only. Thus, formula (7) becomes

$$\frac{\Delta T_m}{\Delta T_0} = 6.2p \frac{\rho_A}{\rho_{ms}} \cdot \frac{c_A}{c_{ms}} \cdot \frac{U_0}{U_m} \cdot \frac{r_0^2}{b^2}$$

For the design of heat exchangers with fluidization beds, it is worthwhile to have the bed operate in the local spouting mode, i.e., to make the ratio $x_j/l_b \geq 0.8$. An almost complete temperature relaxation within the jet zone will thus be ensured. This requires an appropriate selection of the gas distributor. If a 90% relaxation is regarded sufficient, then the height of the active zone can be roughly found from the following formula based on expression (9):

$$x_a = 7.85 \frac{r_0}{C_{in}} \sqrt{\frac{c_A}{c_{A'}} \cdot \frac{U_0}{U_l}} \quad (10)$$

It is necessary here to maintain the ratio $x_j/l_b \geq 0.8$.

In other circumstances, when fluidization apparatus is designed for other applications and the bed height is selected on the basis of other criteria, a calculation of the heat transfer must take into account the existence of two heat-transfer zones: a jet zone and a bubble zone.

The preceding discussion applies, in our view, not only to heat exchangers but also to mass exchangers but also to mass exchangers with fluidization beds.

NOTATION

U	is the jet velocity at any point;
U_0	is the initial jet velocity;
U_m	is the jet velocity at the axis;
U_l	is the free lift velocity;
b	is the total thickness of the dynamic boundary layer;
T	is the temperature at any point;
T_m	is the temperature at the jet axis;
T_0	is the initial temperature;
T_b	is the bed temperature;
T_j	is the temperature at the tip of the jet;
θ	is the superheat;
C_{in}	is an empirical coefficient for an anisothermal jet;
r_0	is the initial jet radius;
r	is the instantaneous jet radius;
ρ_{ms}	is the mean-over-the-section jet density;
ρ_A	is the air density;
$\rho_{A'}$	is the density in the air-solid particles zone;
l_b	is the bed height;
x	is the distance from the nozzle edge to a certain cross section;
x_j	is the length of a jet;
x_a	is the length of the active zone;
$Ga = gd_e^3/\nu^2$	is the Galileo number;
p	is the coefficient of relaxation along the jet axis;
W	is the fluidization number;

c_{ms} is the mean-over-the-section specific heat;
 c_A is the specific heat of air;
 $c_{A'}$ is the specific heat in the air-solid particles zone;
 $\Delta T = T - T_b$;
 $\Delta T_m = T_m - T_b$;
 $\Delta T_0 = T_0 - T_b$.

LITERATURE CITED

1. N. I. Gel'perin, V. G. Ainshtein, and V. B. Kvasha, Principles of Fluidization Engineering [in Russian], Khimiya (1967).
2. N. A. Shakhova, Doctor's Dissertation [in Russian], MIKhM, Moscow (1966).
3. N. A. Shakhova, Transactions of the Scientific-Technical Conference in Moscow Institute of Chemical Apparatus Design [in Russian], Moscow (1966).
4. N. A. Shakhova, Heat and Mass Transfer in Flowing Disperse Media [in Russian], Vol. 5, Minsk (1968).
5. S. S. Zabrodskii, Hydrodynamics and Heat Transfer in a Fluidization Bed [in Russian], Izd. GÉI (1963).
6. N. A. Shakhova and G. A. Minaev, Inzh.-Fiz. Zh., 19, Nos. 5 and 6 (1970).
7. P. N. Rowe, B. A. Partridge, and E. Lyall, "Cloud formation around bubbles in gas fluidized beds," Chem. Engng. Sci., 19, No. 12 (1964).
8. R. Toei and R. Matsumo, "Gas interchange between a bubble and the continuous phase in gas-solid fluidized beds," Memo. Fac. Engng., Kyoto Univ. (1968).
9. G. N. Abramovich, Theory of Turbulent Jets [in Russian], Fizmatgiz (1960).
10. G. Schlichting, Theory of the Boundary Layer [Russian translation], Nauka (1969).